



BUNDLE: A program for building the transmembrane domains of G-protein-coupled receptors

Marta Filizola^{a,b}, Juan J. Perez^{a,*} & Maria Cartenì-Farina^b

^a*Departament d'Enginyeria Química, UPC, ETS d'Enginyers Industrials, Avenue Diagonal 647, E-08028 Barcelona, Spain;* ^b*Centro di Ricerca Interdipartimentale di Scienze Computazionali e Biotecnologiche (CRISCEB), Seconda Università degli Studi di Napoli, Via Costantinopoli 16, I-80138 Napoli, Italy*

Received 25 April 1997; Accepted 26 September 1997

Key words: GPCR, novo modeling, rhodopsin, transmembrane domains, receptors

Summary

The only information available at present about the structural features of G-protein-coupled receptors (GPCRs) comes from low resolution electron density maps of rhodopsin obtained from electron microscopy studies on 2D crystals. Despite their low resolution, maps can be used to extract information about transmembrane helix relative positions and their tilt. This information, together with a reliable algorithm to assess the residues involved in each of the membrane spanning regions, can be used to construct a 3D model of the transmembrane domains of rhodopsin at atomic resolution. In the present work, we describe an automated procedure applicable to generate such a model and, in general, to construct a 3D model of any given GPCR with the only assumption that it adopts the same helix arrangement as in rhodopsin. The present approach avoids uncertainties associated with other procedures available for constructing models of GPCRs based on a template, since sequence identity among GPCRs of different families in most of the cases is not significant. The steps involved in the construction of the model are: (i) locate the centers of the helices according to the low-resolution electron density map; (ii) compute the tilt of each helix based on the elliptical shape observed by each helix in the map; (iii) define a local coordinate system for each of the helices; (iv) bring them together in an antiparallel orientation; (v) rotate each helix through the helical axis in such a way that its hydrophobic moment points in the same direction of the bisector formed between three consecutive helices in the bundle; (vi) rotate each helix through an axis perpendicular to the helical one to assign a proper tilt; and (vii) translate each helix to its center deduced from the projection map.

Introduction

G-protein-coupled receptors (GPCRs) are a large group of integral proteins of pivotal importance, directly involved in the transmission of signals to the interior of the cell. These receptors consist of a single polypeptide chain containing seven hydrophobic domains looping back and forth across the lipidic membrane [1,2]. Analysis of the hydrophobicity profile of these transmembrane domains computed from their amino acid sequence suggests that these domains adopt helical secondary structures [3]. Finally, helices pack in a bundle, arranged to exhibit a hydrophobic

outer surface facing the lipidic membrane and a hydrophilic inner surface that originates a binding pocket in the interior.

To date, detailed structural information of membrane proteins is very scarce. This is due to the difficulties associated with their isolation in the quantities demanded by structural analysis. Furthermore, it is notoriously difficult to obtain crystals of these proteins suitable for structural analysis by X-ray diffraction. Rhodopsin is the only GPCR structurally characterized to date from electron microscopy analysis of 2D crystals [4,5]. Unfortunately, the resolution of the two structures available is too low (9 and 7 Å, respectively) to furnish detailed structural information necessary

* To whom correspondence should be addressed.

to understand ligand–receptor interactions. However, the electron density projection maps directly confirm that the transmembrane regions are arranged in a seven-helix bundle, providing information about its relative orientation. Molecular modeling techniques can make use of this information together with the results obtained from biophysical and mutation studies of GPCRs or structure–activity relationship studies to construct models of these proteins at the atomic level. These models are aimed at providing new insights into the 3D structure of these receptors, increasing our level of understanding of ligand–receptor interactions.

In recent years, the elaboration of 3D models of GPCRs has challenged many researchers [6–32]. Early models of these proteins were constructed by sequence homology modeling using bacteriorhodopsin as a template. Bacteriorhodopsin is a membrane protein exhibiting seven transmembrane domains, that is not a GPCR and whose atomic coordinates were deduced from the electron density projection map recorded at 3.5 Å resolution from electron microscopy studies on 2D crystals [33]. However, the lack of significant sequence identity between bacteriorhodopsin and GPCRs, together with the recent findings of substantial differences with rhodopsin in its helix arrangement, directed modeling studies to construct GPCRs without using bacteriorhodopsin as a template. One of the alternative routes is to use rhodopsin as a template. However, since its atomic coordinates are not available, it is first necessary to construct an atomic model of it. Some of the models proposed have been generated by sequence homology using the atomic coordinates of bacteriorhodopsin and followed by a manual rearrangement of the helices using computer graphics to comply with the electron density projection map of rhodopsin. The resulting structure is then being used as a template for modeling other GPCRs. Unfortunately, these models have a limited usefulness since (i) there is not significant sequence identity between GPCRs of different families; and (ii) transmembrane regions have different lengths in diverse GPCRs. These two issues make questionable the construction of GPCRs by homology modeling. On the other hand, procedures to construct *de novo* models of a given GPCR have also been proposed. One of such approaches has successfully employed sequence divergence analysis to construct several GPCRs [8]. However, the procedure has a limited applicability since it requires the comparison of a large number of sequences sharing a sequence identity of 60% or higher. Alternatively, a rule-based approach has also

been proposed [15]. Models are constructed using a simulated annealing protocol, imposing geometrical restraints inferred from all experimental or theoretical studies of the receptor. Despite the procedure being very robust, its use is limited to the availability of experimental and theoretical results on a given GPCR or to the transferability of known results of other GPCRs to the receptor being modeled.

In the present work, a general procedure to construct *de novo* the transmembrane domains of any given GPCR is proposed. The method does not require the use of a template and avoids the requirements of the sequence divergency analysis procedure. Construction of the transmembrane domains of the receptor is based on the assumption that the transmembrane helices are arranged in a seven-helix bundle with the same geometrical disposition as exhibited by rhodopsin. In this procedure, each helix is treated as a rigid object and global manipulations on the helix are induced on every atom through a local coordinate framework defined on the center of the helix. The steps involved in the construction of the receptor are: (i) location of the centers of the helices, deduced from the low-resolution electron density map; (ii) computation of the tilt of each helix, based on the elliptical shape exhibited by the helix on the projection map; (iii) definition of a local coordinate axis for each of the helices; (iv) orientation of the seven helices in an antiparallel fashion; (v) rotation of each helix through the helical axis in such a way that its hydrophobic moment points in the same direction of the bisector formed between three consecutive helices in the bundle; (vi) rotation of each helix through an axis perpendicular to the helical one to provide the proper tilt; and (vii) translation of each helix to its center as deduced from the projection map. All these steps are described below and can be performed in an automatic fashion using the program BUNDLE, developed in our laboratory.

Definition of a helix local coordinate system

The very first information required to model GPCRs is to decide the way in which the helices are arranged in the bundle. This information cannot be deduced from the bovine rhodopsin electron density projection map. Indeed, since the map exhibits two symmetry-related images, both of which may represent a view from the same side of the membrane, there are 10 080 ($2 \times 7!$) possible ways to assign them. In the present work, helices were assigned following the assump-

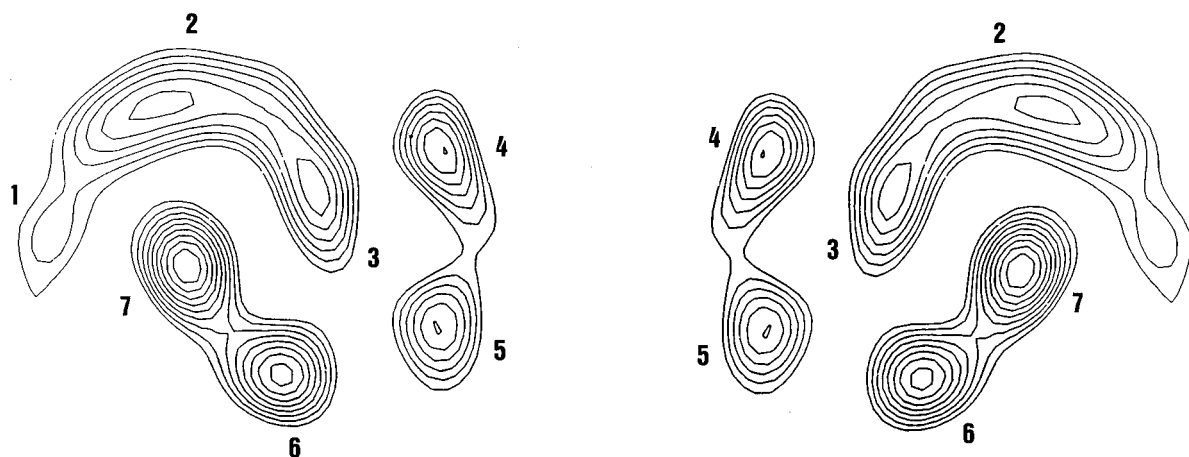


Figure 1. Schematic representation of the asymmetric unit of the rhodopsin electron density projection map. Numbering of the helices was carried out following Baldwin's suggestions (see text).

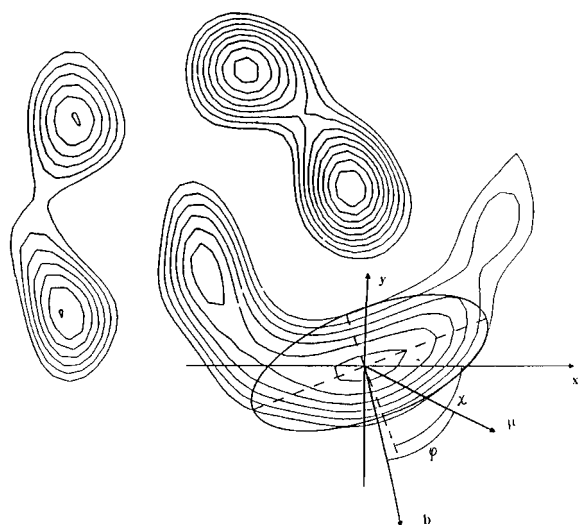


Figure 2. Illustration of ellipse inscription carried out on top of each of the seven helices. b indicates the direction of the bisector of the angle defined between the centers of the previous, the present and the following helix centers and always defined to face the lipophilic side of the bundle. μ is the hydrophobic moment, ϕ is the angle between μ and b and χ is the angle between the ellipse minor axis and the X-axis.

tions proposed by Baldwin [34], as shown schematically in Figure 1. Combining the low-resolution map of rhodopsin with a detailed analysis of 204 GPCR sequences, together with the analysis of length ranges of the interhelical loops, she was able to fit each helix to the peaks in the projection map of rhodopsin and to propose tentative 3D arrangements of the helices by means of helical wheel projection models. Furthermore, whereas the seven helices of rhodopsin

can be characterized from the electron density map, its sense of orientation (clockwise or counterclockwise) remains unclear. However, the counterclockwise orientation has recently become much more probable, as suggested by the results of a set of mutation experiments [35]. In any case, the algorithm presented in the present work can handle both models.

Ideally, if the bundle were an arrangement of seven regular antiparallel helices, the projection map should be expected to exhibit seven circles. Instead, as shown in Figure 2, an ellipse can be more appropriately defined on top of each helix. In the present modeling approach, we assumed that ellipse eccentricity is only due to the tilt θ of the helix. Inspection of Figure 3 suggests that tilts can be easily computed. Let A be the direction of the Z axis and B the direction of the helical axis according to the tilt of the helix. The ratio between the ellipse principal semi-axis, x , and a half of the length of the helix, ℓ , provides the tangent of the angle of tilt, θ :

$$\theta = \arcsin\left(\frac{2x}{\ell}\right)$$

where the sign of θ is decided upon considerations of the lengths of the loops joining two consecutive helices. Moreover, the direction of the ellipse minor axis defines the rotation axis required to provide the proper tilt to each one of the helices. This direction is characterized by the angle (χ) between this direction and the X-axis (Figure 2). Finally, the points where the two ellipse axis cross, determine the coordinates of the helix centers, assumed to lie in the plane $z=0$. All these parameters are listed in Table 1.

Table 1. Bundle parameters deduced from the 2D electron density map of rhodopsin assuming the coordinate origin placed on the center of helix VI

Helix #	Helix center x,y (Å)	Tilt angle θ (°)	Tilt orientation χ (°)	Bisector vectors x,y (Å)
Helix I	-9.894, -15.714	-9.49	-59.74	-9.435, -0.838
Helix II	0.582, -20.564	16.35	75.96	2.02, -11.366
Helix III	8.148, -12.998	22.67	0.0	5.906, -8.922
Helix IV	17.266, -9.312	15.72	0.0	9.246, -3.353
Helix V	11.252, 1.940	14.62	-15.94	5.602, 11.462
Helix VI	0.0, 0.0	13.86	33.69	-7.936, 8.209
Helix VII	-2.134, -10.282	14.30	5.71	-8.77, 5.775

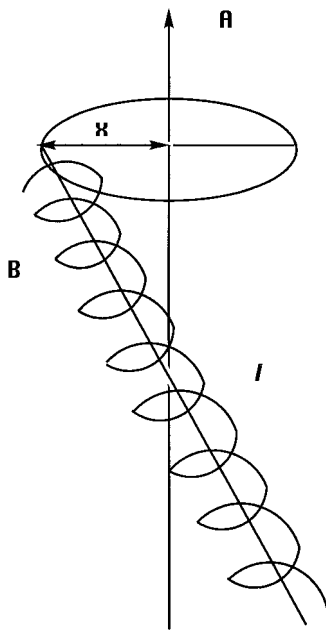


Figure 3. Procedure used to compute the tilt of each helix: x is the ellipse major semi-axis and ℓ is the length of the helix.

Information deduced from the rhodopsin electron density projection map

The first step to be performed to build a GPCR is to accurately assess the sequence of each of the seven transmembrane domains. For this purpose, we make use of the program PHDhtm [36], a neural network system capable of locating the transmembrane helices in integral membrane proteins with 95% accuracy. Its predictions are based on multiple sequence alignment of several GPCRs and have been shown to be very reliable.

Dihedral angles of a regular right-handed α -helix ($\Phi = -57^\circ$, $\Psi = -47^\circ$) are assigned to each of the putative transmembrane polypeptide segments, with the exception of prolines, where $\phi = -65^\circ$. Even though, under these conditions, the helices generated exhibit a kink at the proline residues, they have not had a special treatment in the present procedure. For convenience, side chains were kept in the extended conformation. Subsequently, a local coordinate system is defined. First, the mean position of the helix is calculated from the Cartesian coordinates of all the helix atoms:

$$\bar{x} = \frac{1}{N} \sum_i x_i, \bar{y} = \frac{1}{N} \sum_i y_i, \bar{z} = \frac{1}{N} \sum_i z_i$$

where N is the number of atoms in the helix and x_i , y_i , z_i are the coordinates of atom i . Coordinates of the mean position are subsequently subtracted from those of every atom, resulting in a translation of the helix to a new coordinate system with the mean position as origin.

In order to define a helical coordinate system, a variance matrix is defined as follows:

$$\Delta = \begin{bmatrix} \Delta_{xx} & \Delta_{xy} & \Delta_{xz} \\ \Delta_{yx} & \Delta_{yy} & \Delta_{yz} \\ \Delta_{zx} & \Delta_{zy} & \Delta_{zz} \end{bmatrix}$$

where

$$\Delta_{xy} = \sum_i (x_i - \bar{x})(y_i - \bar{y})$$

This matrix provides an estimation of the dispersion of the atomic coordinates with respect to the mean point computed above. Diagonalization of this matrix yields three orthogonal eigenvectors that, once normalized, are used to define the new local coordinate system. These vectors also define the rotation matrix necessary

to transform the atomic coordinates to the new local coordinate system.

Helix manipulations

Since GPCRs consist of a single polypeptide chain looping back and forth across the lipidic bilayer, transmembrane helical domains must be organized in an antiparallel fashion with the exception of the first and the seventh. Consequently, the first transformation to be performed on the individual helices consists of a 180° turn on helices #2, 4 and 6 to get all the helices in an antiparallel orientation.

Once helices are properly oriented, next the hydrophobic moment μ of each helix is determined. The hydrophobic moment of a helix is computed as the summation of unitary vectors, defined on each residue as the difference of the side-chain mean point coordinates and those of the C^α , and multiplied by the hydrophobic value of the residue as weighting factor [37]:

$$\mu_x = \sum_i \xi_i (x_{is} - x_{i\alpha}), \quad \mu_y = \sum_i \xi_i (y_{is} - y_{i\alpha}),$$

$$\mu_z = \sum_i \xi_i (z_{is} - z_{i\alpha})$$

where ξ_i are the hydrophobicity values of residue i in the Kyte and Doolittle [38] scale and x_{is} , y_{is} , z_{is} are the coordinates of the mean point of the side chain of residue i .

The hydrophobic moment defines the most hydrophobic side of the helix and consequently the one facing the lipidic bilayer. Inspection of the projection map suggests that not all the helices have the same exposure to the lipidic environment, helix #3 being the least exposed. This different exposure can quantitatively be assessed by the value of the angle formed between the centers of three consecutive helices. The larger the angle, the more exposed is the helix to the lipidic phase. The simplest way to use the hydrophobic moment to dictate helix orientation in the bundle is to force it to point in the direction of the bisector of the angle formed between the centers of the previous helix, the one under consideration and the following one deduced from the electron density map. Coordinates of the vectors defining the bisectors referred to the respective local axis of each helix are listed in Table 1. Let j be the angle between the hydrophobic moment μ and the direction of the bisector \mathbf{b} (Figure 2). In

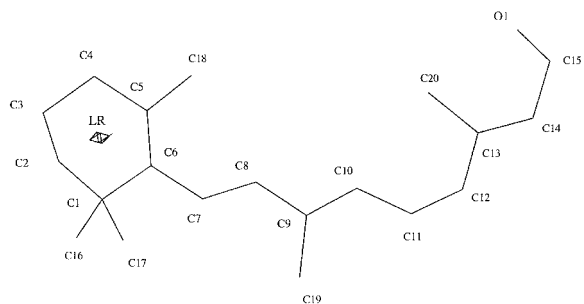


Figure 4. Schematic representation of 11-*cis*-retinal, indicating the atomic labeling.

order to make both vectors point in the same direction, a rotation R of the angle φ around the helical axis should be performed to each helix. However, the need to apply in a subsequent operation a tilt to each helix requires to rotate the helix by an angle $\varphi + \chi$, χ being the angle between the ellipse minor axis and the X axis. Rotation around angle χ will be later subtracted:

$$R = \begin{bmatrix} \cos(\varphi + \chi) & -\sin(\varphi + \chi) & 0 \\ \sin(\varphi + \chi) & \cos(\varphi + \chi) & 0 \\ 0 & 0 & 1 \end{bmatrix}$$

Once helices are transformed, an additional rotation through the minor axis of the ellipse defined on top of each helix needs to be performed to provide the proper tilt. This operation R includes the simultaneous rotation of the tilt angle θ around the ellipse minor axis located on the XY plane and a rotation of $-\chi$ around the Z axis:

$$R = \begin{bmatrix} \cos(-\chi) & -\sin(-\chi) & 0 \\ -\cos \theta \sin(-\chi) & \cos \theta \cos(-\chi) & -\sin \theta \\ \sin \theta \sin(-\chi) & \sin \theta \cos(-\chi) & \cos \theta \end{bmatrix}$$

After this operation is performed, the final step consists of translating the centers of the helices according to the coordinates listed in Table 1.

Results and discussion

The procedure described above has the great advantage of being totally general and can be used to construct a model of any given GPCR. The method provides a completely automated procedure that avoids manual manipulation and does not require to have high identity sequence receptors, necessary for both homology modeling and sequence divergence analysis.

```

1      100
MNGTEGPNFYVPFSNKTGVVRSFPFEARQYYLAEPW QFSMLAAAYMFLIMLGFPINFLTYVTVQHFKIKLRTPLN YILNLAVADLFMVFGGFTTLYTSLH

101      200
GYFVFGPTGCNLEGFATLGGFIALW SLVVLAIERYVVVCKPMSNFRFGEN HAIMGVAFTWVMALACA APPLVGW SRYIPEGMQCSCGIDYYTPHEETNN

201      300
ESFVYMFVVHFIPLIVIFFCYGOLVFTVKEAAAQQQSATTQKAKEFVTRMV IIMVIAELICWLPYAGVAFYIFTHQGSDFGPIFMTIPAFFAKTSAV

301      348
YNIPIYIMMNKQFRNCMVTTLCCKGNPLGDDEASTTVSKTETSQVAPA

```

Figure 5. Amino acid sequence of rhodopsin with the putative transmembrane domains highlighted.

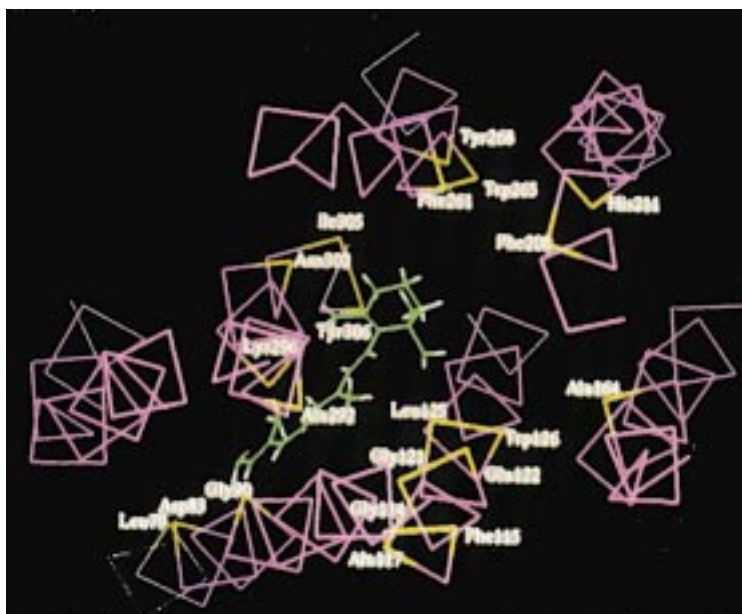


Figure 6. Model of rhodopsin constructed with BUNDLE.

The procedure outlined in the present work represents the simplest approximation to construct GPCRs without using a template. However, there are some considerations that need to be made about the approximations assumed in the present procedure. First, there is no direct evidence that all GPCRs exhibit the same arrangement as rhodopsin. However, it is likely that all of these receptors have evolved from a single ancestral gene and share basic structural and functional features [39]. Second, forcing the direction of the hydrophobic moment to coincide with that of the helix bisector is an approximation that works better for those helices exhibiting large hydrophobic moments. Obviously, helices with small hydrophobic moment are less amphipathic and it will be more difficult to predict their orientation. However, models constructed so far fulfill known experimental results, providing the residues

known to be important for ligand binding oriented to the interior of the receptor. Third, prolines induce a kink in the helices and consequently deviate them from ideality. This may affect the estimation of the tilt assigned to each of the helices, since the observed elliptical shape of a helix on the electron density map can be due to both effects. However, in case there is an overestimation of the tilt, this is corrected during the refinement procedure, since energy minimization proceeds without constraints and, consequently, contacts between helices are easily resolved.

This procedure has successfully been used to generate atomic models of rhodopsin and other GPCRs. The results of applying the procedure to the former system will be briefly discussed below.

Rhodopsin represents a good test case protein, since the procedure outlined above are based on its

projection map and there are a number of experimental studies that provide a wealth of information about the residues directly involved in its interaction with the chromophore. These results can be used to assess the quality of the present model, since these residues should all face the interior of the bundle and, furthermore, they should be located at appropriate distances to interact with its natural ligand 11-*cis*-retinal, shown schematically in Figure 4.

Following the procedure described above, a counterclockwise model for rhodopsin was automatically constructed. The sequence of bovine rhodopsin comprises 348 residues and was fetched from the GenBank. The putative transmembrane segments of rhodopsin were assessed using the profile fed neural network system (PHDhtm) from the EMBL in Heidelberg [36]. Sequences of the transmembrane regions are: helix I, 36–62; helix II, 74–110; helix III, 114–139; helix IV, 152–176; helix V, 203–230; helix VI, 255–279; helix VII, 285–308. Figure 5 shows the sequence of rhodopsin with the putative seven transmembrane regions highlighted. Next, a molecule of 11-*cis*-retinal was manually docked inside the bundle in such a way that the carbonyl oxygen O1 of 11-*cis*-retinal was placed at a distance of about 2 Å from the nitrogen of the Lys²⁹⁶ side chain located in helix VII, following the results of Raman spectroscopy [40] and solid-state NMR [41] studies that suggest a covalent link between Lys²⁹⁶ and 11-*cis*-retinal forming a Schiff base. The resulting model is shown in Figure 6. Those residues known to be involved in the interaction with the ligand from site-directed mutagenesis studies [42–53] are depicted in yellow. These residues are: Leu⁷⁹, Asp⁸³ and Gly⁹⁰ for helix II; Gly¹¹⁴, Phe¹¹⁵, Ala¹¹⁷, Gly¹²¹, Glu¹²², Leu¹²⁵ and Trp¹²⁶ for helix III; Ala¹⁶⁴ for helix IV; Phe²⁰⁸ and His²¹¹ for helix V; Phe²⁶¹, Trp²⁶⁵ and Tyr²⁶⁸ for helix VI; and Ala²⁹², Lys²⁹⁶, Asn³⁰², Ile³⁰⁵ and Tyr³⁰⁶ for helix VII. The model structure of the ligand-opsin complex constructed, exhibits numerous contacts and needs to be refined. For this purpose, the helix bundle has to be subjected to energy minimization without constraints to reach the closest local minimum. Subsequently, the model is subjected to a molecular dynamics calculation with the backbone atoms constrained to fully relax the side chains. Distances between key residues and the chromophore molecule in the average structure are in good agreement with experimental data available. Details of the refined model will be published elsewhere, although the coordinates of the refined model are available upon request from the authors.

Finally, it is important to stress that models generated allow one to make predictions about possible mutations that may importantly influence the binding of different ligands to their receptors as well as modifications on the ligands to make the receptor–ligand interaction more effective. The accuracy of these models can be easily contrasted by comparing their predictions with the results of the large number of pharmacophores described in the literature, deduced from comparison of the molecular properties of series of ligands. Modeling the receptors represents an alternative view of the ligand–receptor interactions and may provide new insights into the design of new ligands based on the consistency of the results achieved. Finally, we expect that the procedure described will help to achieve further insight into the ligand–receptor interactions in GPCRs.

Conclusions

This paper describes a general automated procedure to build the transmembrane regions of GPCRs that does not require to use any protein as template. The method is not hampered by the need of finding several receptors with high sequence homology. The procedure is based on the assumption that all GPCRs adopt the same helix arrangement as observed in the rhodopsin projection electron density map obtained from electron microscopy of 2D crystals. From this map, the location of the seven helix centers as well as their tilts from the elliptical shape exhibited by each helix in the projection map can be measured. The next step consists of assessing the sequence of the transmembrane regions by means of the profile fed neural network system from the EMBL and to construct seven ideal α -helices of these sequences. Next, helices are manipulated according to the following steps: (i) definition of a local coordinate axis for each of the helices; (ii) orientation of them in an antiparallel fashion; (iii) rotation of each helix through the helical axis in such a way that its hydrophobic moment is pointing in the same direction of the bisector formed between three consecutive helices in the bundle; (iv) rotation of each helix through an axis perpendicular to the helical one to assign a proper tilt; and (v) translation of each helix to its center deduced from the projection map. All these steps are performed automatically by a program developed in our laboratory called BUNDLE, available from the authors upon request.

The procedure described was used to model rhodopsin and other GPCRs. The reliability of these models can be assessed either directly by site-directed mutagenesis experiments or indirectly from recognition of the pharmacophore requirements deduced from previous indirect modeling studies. These models can be clearly used to acquire new insights into the ligand-receptor interactions.

Acknowledgements

The authors wish to express their gratitude both to the Italian and Spanish governments for a collaborative research grant HI-1995-0091B between the two laboratories. Financial support from the 'Fondi della Regione Campania (Italia)' is also acknowledged.

References

- Strader, C.D., Fong, T.M., Tota, M.R., Underwood, D. and Dixon, R.A.F., *Annu. Rev. Biochem.*, 63 (1994) 101.
- Watson, S. and Arkininstall, S., *FactsBook*, Academic Press, London, 1994.
- Samatey, F.A., Xu, C. and Popot, J.-L., *Proc. Natl. Acad. Sci. USA*, 92 (1995) 4577.
- Schertler, G.F.X., Villa, C. and Henderson, R., *Nature*, 362 (1993) 770.
- Schertler, G.F.X. and Hargrave, P.A., *Proc. Natl. Acad. Sci. USA*, 92 (1995) 11578.
- Baldwin, J.M., *Curr. Opin. Cell Biol.*, 6 (1994) 180.
- Donnelly, D., *Protein Eng.*, 7 (1994) 645.
- Alkorta, I. and Du, P., *Protein Eng.*, 7 (1994) 1231.
- Brann, M.R., Klimkowski, V.J. and Ellis, J., *Life Sci.*, 52 (1993) 405.
- Cronet, P., Sander, C. and Vriend, G., *Protein Eng.*, 6 (1993) 59.
- Dahl, S.G., Edvardsen, O. and Sylte, I., *Proc. Natl. Acad. Sci. USA*, 88 (1991) 8111.
- De Benedetti, P.G., Menziani, M.C., Fanelli, F. and Cocchi, M., *J. Mol. Struct. (THEOCHEM)*, 285 (1993) 147.
- Fanelli, F., Menziani, M.C., Cocchi, A., Leonardi, A. and De Benedetti, P.G., *J. Mol. Struct. (THEOCHEM)*, 314 (1994) 265.
- Fanelli, F., Menziani, M.C., Cocchi, M. and De Benedetti, P.G., *J. Mol. Struct. (THEOCHEM)*, 333 (1995) 49.
- Herzyk, P. and Hubbard, R.E., *Biophys. J.*, 69 (1995) 2419.
- Hutchins, C., *Endocr. J.*, 2 (1994) 7.
- Hibert, M.F., Trump-Kallmeyer, S., Bruinvels, A. and Hoflack, J., *Recept. Mol. Pharmacol.*, 40 (1991) 8.
- Grotzinger, J., Engels, M., Jacoby, E., Wollmer, A. and Strabburger, W., *Protein Eng.*, 4 (1991) 767.
- Livingstone, C.D., Strange, P.G. and Naylor, L.H., *Biochem. J.*, 28 (1992) 7277.
- Trump-Kallmeyer, S., Hoflack, J., Bruinvels, A. and Hibert, M.F., *J. Med. Chem.*, 35 (1992) 3448.
- Yamamoto, Y., Kamiya, K. and Terao, S., *J. Med. Chem.*, 36 (1993) 820.
- Kyle, D.J., Chakravarty, S., Sinsko, J.A. and Stormann, T.M., *J. Med. Chem.*, 37 (1994) 1347.
- Laakkonen, L.J., Guarnieri, F., Perlman, J.H., Gershengorn, M.C. and Osman, R., *Biochemistry*, 35 (1996) 7651.
- Menziani, M.C., Cocchi, M., Fanelli, F. and De Benedetti, P.G., *J. Mol. Struct. (THEOCHEM)*, 333 (1995) 243.
- Neumuller, M. and Jahnig, F., *Proteins Struct. Funct. Genet.*, 26 (1996) 146.
- Nordvall, G. and Hacksell, U., *J. Med. Chem.*, 36 (1993) 967.
- Pardo, L., Ballesteros, J.A., Osman, R. and Weinstein, H., *Proc. Natl. Acad. Sci. USA*, 89 (1992) 4009.
- Perlman, J.H., Laakkonen, L.J., Guarnieri, F., Osman, R. and Gershengorn, M.C., *Biochemistry*, 35 (1996) 7643.
- Sansom, M.S.P., Son, H.S., Sankaramakrishnan, R., Kerr, I.D. and Breed, J., *Biophys. J.*, 68 (1995) 1295.
- Sylte, I., Edvardsen, O. and Dahl, S.G., *Protein Eng.*, 6 (1993) 691.
- Yamano, Y., Ohyama, K., Kikyo, M., Sano, T., Nakagomi, Y., Inone, Y., Nakamura, N., Morishima, I., Guo, D.F., Hamakubo, T. and Inagami, T., *J. Biol. Chem.*, 270 (1995) 14024.
- Zhang, D.Q. and Weinstein, H., *J. Med. Chem.*, 36 (1993) 934.
- Grigorieff, N., Ceska, T.A., Downing, K.H., Baldwin, J.M. and Henderson, R., *J. Mol. Biol.*, 259 (1996) 393.
- Baldwin, J.M., *EMBO J.*, 12 (1993) 1693.
- Beck-Sickinger, A.G., *Drug Discov. Today*, 1 (1996) 502.
- Rost, B., Casadio, R., Fariselli, P. and Sander, C., *Protein Sci.*, 4 (1995) 521.
- Eisenberg, D., Weiss, R.M. and Terwilliger, T.C., *Nature*, 299 (1982) 371.
- Kyte, J. and Doolittle, R.F., *J. Mol. Biol.*, 157 (1982) 105.
- Attwood, T.K. and Findlay, J.B.C., *Protein Eng.*, 6 (1993) 167.
- Palings, I., Pardeon, J.A., Vandenberg, E., Winkel, C., Lugtenburg, J. and Mathies, R.A., *Biochemistry*, 26 (1987) 2544.
- Smith, S.O., Palings, I., Miley, M.E., Courtin, J., de Groot, H., Lugtenburg, J., Mathies, R.A. and Griffin, R.G., *Biochemistry*, 29 (1990) 8158.
- Cohen, G.B., Oprian, D.D. and Robinson, P.R., *Biochemistry*, 32 (1993) 6111.
- Dryja, T.P., Berson, E.L., Rao, V.R. and Oprian, D.D., *Nat. Genet.*, 4 (1993) 280.
- Nakayama, T.A. and Khorana, H.G., *J. Biol. Chem.*, 265 (1990) 15762.
- Nakayama, T.A. and Khorana, H.G., *J. Biol. Chem.*, 266 (1991) 4269.
- Nathans, J., *Biochemistry*, 29 (1990) 9746.
- Neitz, M., Neitz, J. and Jacobs, G.H., *Science*, 252 (1991) 971.
- Oprian, D.D., *J. Bioenerg. Biomembr.*, 24 (1992) 211.
- Rao, V.R., Cohen, G.B. and Oprian, D.D., *Nature*, 367 (1994) 639.
- Ridge, K.D., Bhattacharya, S., Nakayama, T.A. and Khorana, H.G., *J. Biol. Chem.*, 267 (1992) 6770.
- Robinson, P.R., Cohen, G.B., Zhukovsky, E.A. and Oprian, D.D., *Neuron*, 9 (1992) 719.
- Zhukovsky, E.A. and Oprian, D.D., *Science*, 246 (1989) 928.
- Zvyaga, T.A., Fahmy, K. and Sakmar, T.P., *Biochemistry*, 33 (1994) 9753.